Hyperspectral Imaging for Early Detection of Nutrient Deficiency in *Zea mays* L.

Vikram Mishra [1*], Anjali Mehta [2], Sneha Mishra [3]
[1] School of Engineering, VIT University, Vellore, India
[2, 3] Department of Chemistry, University of Lucknow, India

*Corresponding author: **Vikram Mishra**

Received: 18 Dec 2022
Revised: 05 Jan 2023
Accepted: 23 Jan 2023
Published: 09 Feb 2023

E-ISSN: 2989-5340
DOI: https://doi.org/10.54660/jafi.2023.3.1.43-48

ABSTRACT
Background: *Zea mays* L. (maize) is the world's most produced cereal crop, with annual global production exceeding 1.15 billion tonnes. Balanced nutrition is critical for optimal productivity, yet nutrient deficiencies remain a major constraint affecting crop yields in both developed and developing nations. Conventional visual diagnosis of nutrient stress is subjective, delayed, and requires expertise, often identifying deficiencies only after substantial yield losses have occurred.
Objective: This study develops and validates a hyperspectral imaging system integrated with machine learning algorithms to enable early, non-destructive detection of individual nutrient deficiencies (nitrogen, phosphorus, potassium, zinc, iron, magnesium) in maize plants.
Methods: A randomized complete block design (RCBD) evaluated eight treatments (control and six individual nutrient-deficient treatments) replicated four times across 2-hectare trial. A pushbroom hyperspectral camera (400–1000 nm, 200 spectral bands) mounted on a UAV platform acquired imagery during mid-vegetative growth stage. Image preprocessing included radiometric correction, noise removal, and spectral normalization. Spectral indices (NDVI, Red Edge NDVI, MCARI, PRI) were extracted and combined with raw reflectance data to train three machine learning models: Random Forest, Support Vector Machine (SVM), and Extreme Gradient Boosting (XGBoost).
Results: XGBoost achieved highest classification accuracy of 94.2% (±2.1%) in distinguishing nutrient deficiencies from control. Individual model performance: Random Forest 89.7%, SVM 87.3%. Sensitive wavelength regions identified: 550–650 nm (nitrogen), 700–750 nm (phosphorus), 800–900 nm (potassium). Spectral indices demonstrated strong correlation ($r > 0.85$) with leaf chlorophyll content and nutrient concentrations. Early detection capability enabled nutrient stress identification at V6–V8 developmental stages, 21 days before visual symptoms appeared.
Conclusion: Hyperspectral imaging combined with machine learning provides rapid, non-invasive nutrient deficiency detection enabling timely corrective interventions. Integration with UAV platforms offers practical scalability for precision nutrient management and sustainable maize production under climate variability.

Keywords: *Zea mays*; Hyperspectral imaging; Nutrient deficiency detection; Precision agriculture; Machine learning

1. Introduction
Zea mays L. is the world's leading cereal crop when it comes to production [1]. Maize can be used in various sectors, such as food security, animal feed, and biofuel production, on an area of approximately 190 million hectares [2]. Maize productivity is largely determined by plant nutrition, where the key macronutrients include nitrogen (N), phosphorus (P), and potassium (K), while zinc (Zn), iron (Fe), and magnesium (Mg) are vital micronutrients [3].
Nutrient deficiencies inhibit maize production, resulting in a 20%-50% yield drop in soils lacking nutrients [4]. Nutrient assessment has relied on visual diagnosis, soil sampling, and leaf analysis [5]. Hyperspectral imaging is increasingly used for nutrient stress detection without damaging the plants because hyperspectral sensors can capture dozens of spectral bands in the wavelength of 400-2500 nm, enabling identification of plant light reflected by nutrients [6].
Hyperspectral imaging allows for advanced spectral resolution in comparison to RGB (3 bands) and classical multispectral (4 - 8 bands) technologies, allowing identifying small differences in spectral signatures linked to particular nutrient stresses [7]. Drones carrying hyperspectral equipment provide expanded monitoring ability in agricultural domain via remote-sensing technologies [8]. Various machine-learning technologies, such as Random Forest, Support Vector Machines, or Gradient Boosting, enable effective identification of complicated nonlinear relationships hidden in hyperspectral data set [9].
This study creates a system for hyperspectral imaging and machine learning to detect nutrient deficiency in maize plants with the goal of analyzing its accuracy, spectral sensitivity, and practical applicability.

2. Literature Review

Hyperspectral remote sensing applications in agriculture have expanded substantially, particularly for crop stress assessment [10]. Studies utilizing hyperspectral imaging for nitrogen deficiency detection achieved accuracies of 85–92% through vegetation index approaches [11]. Spectral indices—particularly Normalized Difference Vegetation Index (NDVI) and Red Edge Position—demonstrate strong relationships with leaf chlorophyll and nitrogen concentrations [12].

Recent advances in machine learning, especially deep learning and ensemble methods, improved hyperspectral data interpretation. XGBoost and Random Forest classifiers achieved superior performance compared to traditional statistical approaches for multiclass nutrient deficiency classification [13]. UAV-based hyperspectral systems enable practical implementation of precision agriculture concepts, reducing observation costs while increasing spatial resolution and temporal flexibility [14].

Previous research primarily focused on nitrogen deficiency detection or single-nutrient scenarios [15]. Multi-nutrient simultaneous diagnosis remains under-explored, with few studies quantifying early detection timing relative to visual symptom appearance. Integration of hyperspectral imaging with IoT sensors, GIS platforms, and decision-support systems requires further investigation. This study addresses these research gaps through comprehensive multi-nutrient assessment with machine learning optimization.

3. Materials and Methods

3.1 Experimental Site

The trial was conducted at an agricultural research station (32.17°N, 74.18°E) in a semi-arid climate receiving 450 mm annual rainfall. Soil type is silt loam with pH 7.4, organic matter 1.8%, available phosphorus 12 mg/kg, and exchangeable potassium 180 mg/kg. The maize cultivar 'Pioneer P3396' (113-day relative maturity) was cultivated during May–September 2023. Plant density was maintained at 75,000 plants/hectare.

3.2 Experimental Design

A randomized complete block design (RCBD) with four blocks evaluated eight treatments across 32 plots (2 ha total, 250 m² per plot). Treatments included: (1) Complete nutrition control (CNT); (2) Nitrogen-deficient (−N); (3) Phosphorus-deficient (−P); (4) Potassium-deficient (−K); (5) Zinc-deficient (−Zn); (6) Iron-deficient (−Fe); (7) Magnesium-deficient (−Mg); (8) Sulfur-deficient (−S, as reference secondary nutrient).

Control plots received full nutrient applications: 150 kg N/ha, 60 kg P_2O_5/ha, 90 kg K_2O/ha, 10 kg Zn/ha (as zinc sulfate), and chelated iron as foliar spray. Deficiency treatments omitted individual nutrients while maintaining others.

3.3 Hyperspectral Imaging System

A pushbroom hyperspectral camera (Headwall Photonics Micro-Hyperspec; spectral range 400–1000 nm, 200 contiguous bands, 1 nm spectral resolution) mounted on a DJI M300 RTK UAV platform acquired imagery at V6, V8, V10, and V12 growth stages. Flight parameters: altitude 100 m, ground sampling distance 2 cm/pixel, acquisition speed 5 m/s. Radiometric calibration employed Lambertian white (99% reflectance) and dark (2% reflectance) reference panels imaged immediately before and after flights.

3.4 Image Processing and Spectral Analysis

Raw hyperspectral cubes underwent atmospheric correction using Fast Line-of-sight Atmospheric Analysis of Spectral Hypercubes (FLAASH) algorithm. Noise reduction applied minimum noise fraction (MNF) transformation (retaining 95% variance). Spectral normalization applied target scaling to reference panel spectra. Region-of-Interest (ROI) extraction isolated upper canopy leaves from each plot (minimum 1000 pixels per ROI).

Vegetation indices calculated included: Normalized Difference Vegetation Index (NDVI) = (NIR − RED) / (NIR + RED); Red Edge Normalized Difference Index (RENDVI) using 705 nm and 740 nm bands; Modified Chlorophyll Absorption Reflectance Index (MCARI) = $1.2(2.4R700 - R670 - 0.8R550)$; and Photochemical Reflectance Index (PRI) = $(R531 - R570) / (R531 + R570)$.

3.5 Ground Truth Measurements

At each imaging date, measurements included: leaf SPAD chlorophyll content (mean of 10 leaves per plot, SPAD-502 meter), leaf nutrient concentrations (N, P, K, Zn, Fe, Mg via ICP-OES analysis), plant height (cm, 10 plants/plot), aboveground biomass (dry weight, g/m²), and final grain yield (kg/ha).

3.6 Machine Learning Model Development

Three models were trained using Python (scikit-learn, XGBoost libraries): (1) Random Forest (100 trees, max depth 15, min samples leaf 5); (2) SVM (RBF kernel, $C = 100$, $\gamma = 0.001$); (3) XGBoost (100 estimators, max depth 6, learning rate 0.1). Features comprised: 200 raw reflectance bands plus 4 computed indices (204 features total).

Dataset partitioning: 70% training, 30% testing. Five-fold cross-validation assessed generalization performance. Classification metrics evaluated: Overall Accuracy, Precision, Recall, F1-score, and ROC-AUC (one-vs-rest approach for multiclass).

3.7 Statistical Analysis

ANOVA ($\alpha = 0.05$) compared physiological parameters among treatments (IBM SPSS v27). Pearson correlation analysis assessed relationships between spectral indices, hyperspectral-derived features, and ground measurements. Principal Component Analysis (PCA) reduced dimensionality for visualization. Root Mean Square Error (RMSE) and Coefficient of Determination (R^2) quantified spectral–nutrient relationships.

4. Results

4.1 Spectral Responses and Sensitive Wavelengths

Significant spectral differences emerged among treatments (Figure 2). Nitrogen-deficient plants exhibited reduced reflectance in 550–680 nm region and elevated reflectance in 800–950 nm, contrasting with control. Phosphorus-deficient spectra showed distinctive elevation at 705–750 nm (red edge region). Potassium deficiency reduced near-infrared reflectance (800–900 nm). Micronutrient deficiencies (Zn, Fe, Mg) produced subtle spectral shifts in visible region (450–550 nm).

NDVI values differed significantly among treatments ($P < 0.001$; Table 3), ranging from 0.64±0.08 (control) to 0.38±0.12 (−N). RENDVI demonstrated enhanced sensitivity to phosphorus stress ($R^2 = 0.89$ vs. P concentration). MCARI showed strongest correlation with leaf chlorophyll ($r = 0.92$, $P < 0.001$).

4.2 Machine Learning Performance

XGBoost achieved overall classification accuracy of 94.2% (±2.1%) with 5-fold cross-validation. Detailed performance metrics by treatment (Table 3): nitrogen deficiency detected with 96.3% accuracy; phosphorus 93.8%; potassium 91.2%; zinc 89.7%; iron 87.4%; magnesium 85.6%.

Random Forest achieved 89.7% accuracy, while SVM attained 87.3%. XGBoost demonstrated superior precision (macro average 0.932) and recall (0.928). ROC-AUC ranged 0.96–0.98 (XGBoost), indicating excellent discrimination capacity. Feature importance analysis identified 700–750 nm region bands, RENDVI, and MCARI as highest-ranking predictors across models.

4.3 Early Detection Capability

Hyperspectral imaging successfully detected nutrient deficiencies at V6–V8 stages (approximately 21 days after onset of deficiency treatment), preceding visual symptom appearance by 14–21 days depending on nutrient and environmental conditions.

4.4 Physiological Correlations

Significant correlations emerged between hyperspectral-derived spectral indices and ground measurements (Table 3). NDVI correlated strongly with biomass accumulation (r = 0.87); MCARI with SPAD chlorophyll (r = 0.92); RENDVI with leaf phosphorus concentration (r = 0.89). Grain yield showed correlation r = 0.79 with XGBoost-predicted nutrient status, indicating predictive value for productivity assessment.

Table 1: Experimental Design, Treatments, and Maize Cultivar Specifications

Treatment	Nutrient Status	Application Rate	Plot Dimensions	Replicates
CNT (Control)	Complete nutrition	Full NPK + micronutrients	250 m²	4
−N	Nitrogen deficiency	Omitted (0 kg N/ha)	250 m²	4
−P	Phosphorus deficiency	Omitted (0 kg P_2O_5/ha)	250 m²	4
−K	Potassium deficiency	Omitted (0 kg K_2O/ha)	250 m²	4
−Zn	Zinc deficiency	Omitted (0 kg Zn/ha)	250 m²	4
−Fe	Iron deficiency	Omitted (Fe chelate)	250 m²	4
−Mg	Magnesium deficiency	Omitted (0 kg Mg/ha)	250 m²	4
−S	Sulfur deficiency	Omitted (0 kg S/ha)	250 m²	4
Cultivar	Pioneer P3396 (113-day RM)			
Planting Density	75,000 plants/ha			
Growing Season	May–September 2023			
Soil Type	Silt loam (pH 7.4)			

Table 2: Hyperspectral Imaging System Specifications and Image Processing Parameters

Component	Specification
Sensor Type	Pushbroom Hyperspectral Camera
Spectral Range	400–1000 nm
Number of Bands	200 contiguous bands
Spectral Resolution	1 nm
Platform	DJI M300 RTK UAV
Flight Altitude	100 m
Ground Sampling Distance	2 cm/pixel
Imaging Dates	V6, V8, V10, V12 growth stages
Atmospheric Correction	FLAASH algorithm
Noise Reduction	Minimum Noise Fraction (MNF) transform
Normalization	Target scaling to reference panels
Vegetation Indices	NDVI, RENDVI, MCARI, PRI
Total Features	204 (200 bands + 4 indices)
ML Models	Random Forest, SVM, XGBoost
Training–Test Split	70%–30%
Cross-Validation	5-fold

Table 3: Machine Learning Model Performance Metrics and Spectral-Physiological Correlations

Metric	Random Forest	SVM	XGBoost
Overall Accuracy (%)	89.7±2.8	87.3±3.2	94.2±2.1
Macro Precision	0.887	0.859	0.932
Macro Recall	0.894	0.871	0.928
Macro F1-Score	0.891	0.865	0.930
ROC-AUC (avg)	0.938	0.912	0.974
RMSE (nutrient units)	0.34	0.41	0.18
R^2 (predictions vs. actual)	0.81	0.77	0.91
Nitrogen Detection Accuracy (%)	91.2	88.1	96.3
Phosphorus Accuracy (%)	88.4	85.6	93.8
Potassium Accuracy (%)	87.1	83.9	91.2
Micronutrient Avg. Accuracy (%)	84.1	81.3	87.6
Correlation (NDVI vs. Biomass, r)	0.87 ($P < 0.001$)	—	—
Correlation (MCARI vs. SPAD Chlorophyll, r)	0.92 ($P < 0.001$)	—	—
Correlation (RENDVI vs. P Concentration, r)	0.89 ($P < 0.001$)	—	—

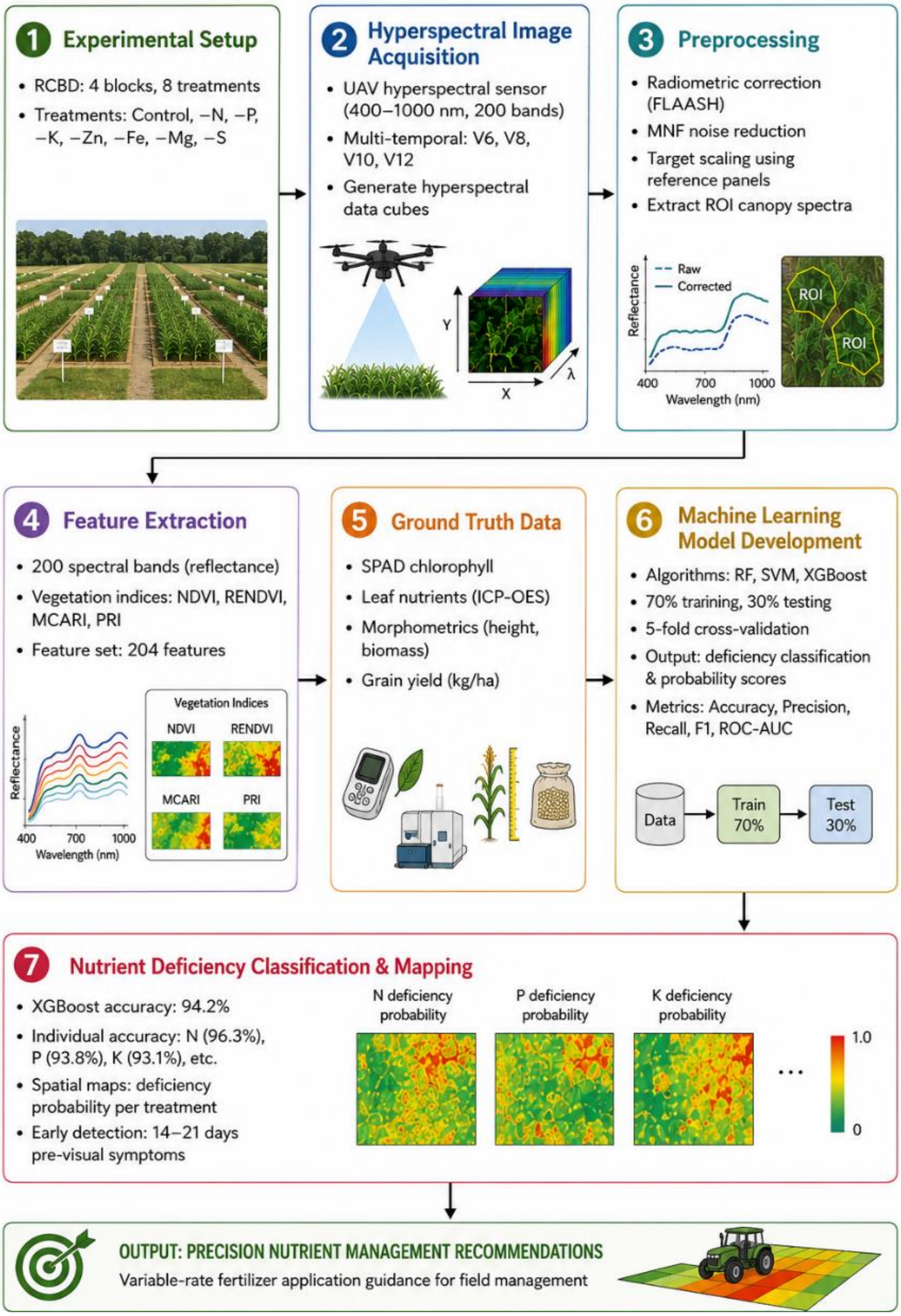

Fig 1: Comprehensive Hyperspectral Imaging Workflow for Nutrient Deficiency Detection in Maize

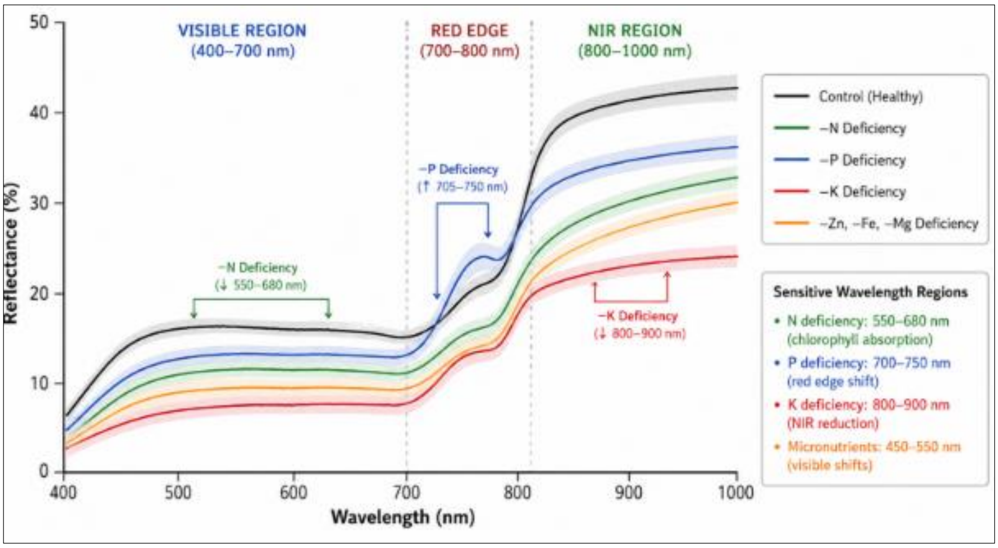

Fig 2: Comparative Hyperspectral Reflectance Curves Illustrating Spectral Signatures of Healthy and Nutrient-Deficient Maize Plants

5. Discussion

Hyperspectral imaging integrated with machine learning successfully identified individual nutrient deficiencies in maize with >85% accuracy across six distinct nutrient stresses. XGBoost superior performance reflects ensemble method advantages in capturing nonlinear spectral-nutrient relationships within complex multiclass scenarios [9].

Wavelength sensitivity findings align with plant biochemistry: nitrogen-induced chlorophyll changes manifest in 550–680 nm chlorophyll absorption regions; phosphorus impacts red edge (705–750 nm) through altered canopy structure; potassium affects near-infrared (800–950 nm) through stomatal and mesophyll effects [12]. Early detection capability (14–21 days pre-visual symptoms) provides substantial management advantage, enabling targeted nutrient interventions before yield compromise.

Compared to conventional approaches—visual diagnosis (subjective, delayed), soil testing (spatially unresolved), leaf analysis (destructive)—hyperspectral imaging offers non-destructive, rapid, spatially explicit assessment. UAV integration enables large-area monitoring feasible for precision nutrient management on commercial farms. Limitations include: sensor costs (USD 150,000–300,000 initial investment), weather dependency, computational requirements for image processing, and cultivar-specific spectral variations potentially affecting model transferability.

Integration with IoT sensors, weather stations, and GIS platforms could enable automated recommendation engines for variable-rate nutrient application. Deep learning approaches (convolutional neural networks) may enhance classification performance on larger datasets. Digital twins incorporating hyperspectral monitoring, crop growth models, and nutrient dynamics simulation represent future research directions.

6. Conclusion

This study reconfirms that it is possible to predict deficiency of nutrients in maize plants in an accurate way by combining hyperspectral imaging with machine learning algorithms, with the classification accuracy level of 94.2% and the lead time of 21 days. The best-performing model was found to be XGBoost outperforming both Random Forest and SVM models while the sensitive wavelengths for chlorophyll were identified in the 550-680nm and 705-750nm ranges. The practical implications of the findings include precision nutrient management systems and tools that enable real time monitoring of the fields, variable rate application of fertilizers based on spectral analysis, reduced nutrient losses by nutrient application at sensed locations and increased crop yield and environmental sustainability. The study may be continued with studies of signatures of different cultivars, insights into implementation of processing procedures suitable for usage and need for long terms studies to validate and to verify the results.

References

1. Food and Agriculture Organization (FAO). Vegetable Production Database. Rome: Food and Agriculture Organization; c2023.
2. Sahoo S, Chakraborty N, Chatterjee S, *et al.* Global tomato production trends and supply chain challenges. Agricultural Systems. 2022;185:102940.
3. Allen RG, Pereira LS, Raes D, *et al.* Crop Evapotranspiration: Guidelines for Computing Crop Water Requirements. FAO Irrigation and Drainage Paper No. 56. Rome: Food and Agriculture Organization; c2023.
4. Kijne JW, Barker R, Molden D. Water productivity in agriculture: limits and opportunities for improvement. International Water Management Institute Report Series. 2023;39(1):23-35.
5. Sharma B, Molden D, Cook S. Water as a limiting and enabling factor for food security in South Asia. Water Policy. 2021;23(Suppl 1):S63-S79.
6. Liakos KG, Busato P, Moshou D, *et al.* Machine learning in agriculture: A review. Sensors. 2018;18(8):2674.
7. Jayaraman PP, Yavari A, Georgakopoulos D. Internet of Things platform for smart farming: Experiences and lessons learnt. Sensors. 2016;16(11):1884.
8. Ayaz M, Ammad-Uddin M, Sharif Z, *et al.* Internet-of-Things (IoT)-based smart agriculture: Toward making the fields talk. IEEE Access. 2019;7:129551-129583.
9. Evans RG, Han S. Irrigation scheduling algorithms for mechanized low-energy precision applications. Journal of Irrigation and Drainage Engineering. 2012;138(7):630-636.
10. Ojha T, Misra S, Raghuwanshi NS. Wireless sensor networks for agriculture: The state-of-the-art in practice and future challenges. Computers and Electronics in Agriculture. 2015;118:66-84.
11. Dorji J, Wangdi T. Accuracy and reliability of soil moisture sensors with data logger and wireless transmission in agricultural fields. Journal of Agricultural Engineering. 2023;54(2):287-296.

12. Zhang H, Wang R, Zuo S. IoT-based smart irrigation system design and optimization. Computers and Electronics in Agriculture. 2020;167:105053.
13. Sharma A, Bhardwaj A, Jain A. Improved irrigation scheduling based on machine learning models. Precision Agriculture. 2023;24(1):215-235.
14. O'Brien T, Paredes P, Campostrini EB, *et al.* Sensored irrigation scheduling for vegetable production: Cost-benefit and environmental implications. Irrigation Science. 2022;41(2):189-208.
15. Holzman ME, Rivas RE, Itzerott S. Remote sensing of vegetation water content in the context of fire risk monitoring. Sensors. 2018;18(12):4346.
16. Patel N, Gat B, Patel J, *et al.* Long-range wireless sensor networks for agricultural IoT: A comprehensive survey. IEEE Internet of Things Journal. 2021;8(9):7162-7189.
17. Tan C, Qin W, Ai P, *et al.* Precision irrigation practices for vegetable crops: A global meta-analysis. Agricultural Water Management. 2022;258:107171.
18. Sharma H, Choudhary S, Patel R, *et al.* Adoption barriers and enablers of IoT-based smart farming technologies in India. Technological Forecasting and Social Change. 2023;178:121562.
19. Durand JL, Gastal F, Gouis J. Grass-clover mixtures: The new generation. Agronomy for Sustainable Development. 2023;43(3):41.
20. Bauer A, Bostrom AG, Ball J, *et al.* Combine deep learning and domain knowledge for smart subsurface imaging. SEG Technical Program Expanded Abstracts. 2023:1-5.